A new approach for estimating the complex permittivity of powdered dielectrics using a rectangular waveguide in the X-band

Omaima Talmoudi[1,*], *Lahcen* Ait Benali[2], *Jaouad* Terhzaz[2], *Abdelwahed* Tribak[1], and *Tomas* Fernandez Ibañez[3]

[1]INPT, Rabat, Morocco
[2]CRMEF CS, Casablanca, Morocco
[3]Universidad de Cantabria, Santander, Spain

Abstract. This paper introduces a new method for estimating the complex permittivity of powdered dielectric materials using a rectangular waveguide. The measurement configuration is based on a multilayer structure in which the powder sample is enclosed between two resin plugs of known complex permittivity. The electromagnetic response of the system is modeled analytically by solving the direct problem under TE_{10} mode propagation and calculating the reflection coefficient S_{11}. To determine the unknown permittivity of the powder, an inverse problem is solved using the Nelder-Mead optimization algorithm implemented via the `fmin` function in Python. The approach iteratively minimizes the difference between calculated and measured S_{11} parameter in the X-band frequency range. Intermediate validation steps with air and resin-only configurations confirm the accuracy of the model. The proposed method provides an accurate and efficient technique for characterizing granular dielectric materials.

1 Introduction

Dielectric powders are becoming widely used in microwave and radio frequency applications due to their tunable electromagnetic properties and compatibility with composite materials. However, the accurate characterization of these materials is still challenging. Unlike bulk solids, powders consist of discrete particles with air gaps in between. Powders are highly sensitive to packing density, moisture content, and interfacial effects [1]. These properties can greatly affect their interaction with electromagnetic fields, particularly in the microwave region.

Many sensors, radars, and communications systems operate in the X-band, and reliable characterization is particularly important [2]. The complex permittivity of a material, both its real and imaginary parts, is crucial to comprehending its absorption, reflection, or transmission of electromagnetic energy in this frequency range [3, 4]. However, the loose structure of the powdered materials complicates the measuring process [5]. Among several methods available, waveguide based techniques have a number of advantages. They are broadband, non-destructive, and rely on well-established field distributions. In particular, the rectangular waveguides permit the accurate and reproducible evaluation of the dielectric properties from

*e-mail: omaimatalmoudi@gmail.com

the analysis of the propagation of the dominant TE_{10}mode [6]. Several theoretical models have been developed over the years for the retrieval of permittivity values from the scattering parameters. Classical inversion methods, such as those based on reflection and transmission coefficients have been widely applied to uniform samples of known geometry [7]. Recent approaches have extended this theory to the case of layered media and the case when only reflection data is available, allowing more flexibility and robustness under practical conditions [1, 8].

In addition, some studies have been concerned with powder materials specifically, and proposed methods including corrections for porosity and heterogeneity. These techniques often use effective medium theories to improve the approximation of the true dielectric behavior of granular mixtures [9, 10].

In this work, we present a theoretical approach adapted to the characterization of powdered samples placed in a WR95 rectangular waveguide. The sample is enclosed between two known dielectric layers, forming a multilayer structure. By applying analytical equations describing wave propagation in such layered configurations, the complex permittivity of the powder can be extracted from the measured S_{11} parameter.

2 Theory

2.1 Direct Problem

The electromagnetic behavior of a rectangular waveguide loaded with a three-layer dielectric structure consisting of two resin layers and a central sand layer placed in an air-filled waveguide is theoretically modeled, as shown in Fig. 1.

The structure represents a dielectric structure with known thicknesses for each layer and known permittivities for the resin layers. In contrast, the complex permittivity of the sand layer ε_r is the parameter to be determined.

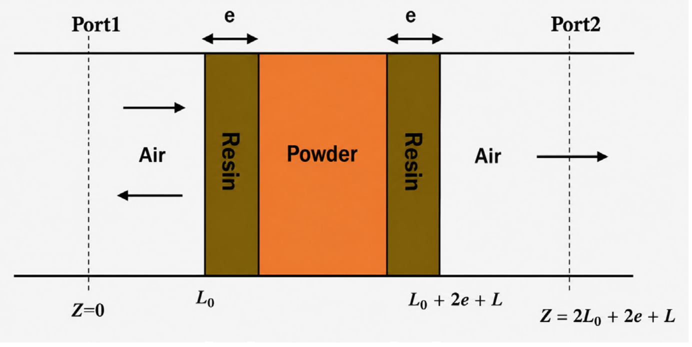

Figure 1. Rectangular waveguide loaded with multilayer dielectric materials.

The multilayer dielectric material is defined along the longitudinal axis z. The first layer is a resin plug with complex permittivity ε_{r1} at the region of $z = L_0$ and $z = L_0 + e$. The central sand layer with unknown complex permittivity ε_r is between $z = L_0 + e$ and $z = L_0 + e + L$. Finally, the second layer of resin is from $z = L_0 + e + L$ to $z = L_0 + 2e + L$. This geometry guarantees that the sample is symmetrically embedded in the waveguide having identical dielectric boundaries on both sides.

The composite electric field in each homogeneous region (air, resin, and sand) is modeled using transmission line theory with forward and backward traveling waves, assuming propagation of TE_{10} mode. Propagation constants in each layer are:

$$\gamma_i = jk_0 \sqrt{\varepsilon_{ri} - \left(\frac{\lambda_0}{\lambda_c}\right)^2} \tag{1}$$

where ε_{ri} is the complex permittivity of region i, $k_0 = \frac{2\pi}{\lambda_0}$ is the free space wave number, and λ_c is the cutoff wavelength of the waveguide.

The multilayer system is analyzed by applying the continuity conditions for the tangential components of the electric and magnetic fields at each interface. The overall scattering parameters, S_{11} and S_{22}, are obtained using a cascade matrix approach that combines the transfer matrices of the individual layers.

For the case of a three-layer structure, such as resin–powder–resin, analytical expressions for the scattering parameters S_{11} and S_{22} can be derived based on the continuity of tangential electromagnetic fields at each interface. These expressions are formulated using the reflection coefficients at the material boundaries and the transmission factors across each layer, incorporating their individual propagation characteristics [1]. The resulting relations are presented in Equations (2) and (3) .

$$S_{11} = \left[\frac{(C_{p1} + C_{s1}T_{p1}^2)(1 + C_{p2}C_{s2}T_{p2}^2) + (C_{p1}C_{s1} + T_{p1}^2)(C_{s2} + C_{p2}T_{p2}^2)T_s^2}{(1 + C_{p1}C_{s1}T_{p1}^2)(1 + C_{p2}C_{s2}T_{p2}^2) + (C_{s1} + C_{p1}T_{p1}^2)(C_{s2} + C_{p2}T_{p2}^2)T_s^2}\right] \times \exp(-2\gamma L_0) \tag{2}$$

$$S_{22} = \left[\frac{-(C_{p2} + C_{s2}T_{p2}^2)(1 + C_{p1}C_{s1}T_{p1}^2) + (C_{p2}C_{s2} + T_{p2}^2)(C_{s1} + C_{p1}T_{p1}^2)T_s^2}{(1 + C_{p1}C_{s1}T_{p1}^2)(1 + C_{p2}C_{s2}T_{p2}^2) + (C_{s1} + C_{p1}T_{p1}^2)(C_{s2} + C_{p2}T_{p2}^2)T_s^2}\right] \times \exp(-2\gamma L_0) \tag{3}$$

The coefficients of reflection and transmission used in the equations (2) and (3) are defined as follows:

The reflection coefficients at the air–resin interfaces are given by:

$$C_{p1} = \frac{Z_p - Z_0}{Z_p + Z_0} \tag{4}$$

$$C_{p2} = \frac{Z_0 - Z_p}{Z_0 + Z_p} \tag{5}$$

The characteristic impedance of the air-filled sections is Z_0, and the characteristic impedance of the resin plugs is Z_p.

The reflection coefficients at the resin powder interfaces are given by:

$$C_{s1} = \frac{Z_s - Z_p}{Z_s + Z_p} \tag{6}$$

$$C_{s2} = \frac{Z_p - Z_s}{Z_p + Z_s} \tag{7}$$

where Z_s is the characteristic impedance of the powder sample and Z_p is the impedance of the resin layers.

Each transmission factor T_i is obtained from the propagation constant as:

$$T_i = e^{-\gamma_i d_i}, \quad i \in \{p1, p2, s\} \tag{8}$$

where d_i is the thickness of layer i and the propagation constant γ_i is computed using Equation (1) with known ε_r for resin and unknown ε_r for sand. This model allows to directly compute S parameters from assumed dielectric constants and thus to formulate an inverse problem for material characterization.

2.2 Inverse Problem

This section describes the method of estimating the complex permittivity of the powder material inserted into a rectangular waveguide. It is composed of three layers with a sand layer in the middle enclosed by two resin plugs. The permittivities of the resin layers are assumed known, while the unknown to be extracted is the complex permittivity of the sand sample.

The estimation is obtained by solving an inverse problem with a numerical optimization method. We use the `fmin` function in Python [11] which implements the Nelder-Mead simplex algorithm a derivative free technique suitable for unconstrained, nonlinear multivariable optimization [7].

The process starts with an initial guess of the complex permittivity, typically $\varepsilon_r' = 2.0$, $\varepsilon_r'' = 0.01$, and is iterated to minimize the following error function [12]:

$$f(\varepsilon_r', \varepsilon_r'') = \sum \left\| S_{ij}^{\text{meas}} - S_{ij}^{\text{model}} \right\|^2 \tag{9}$$

The process improves the estimated values of the real and imaginary parts of the complex permittivity until the scattering parameters modelled are close to the measured data.

3 Numerical Results

The waveguide was prepared with care to match the multilayer dielectric configuration and the appropriate confinement of the powdered sample during measurement. The assembly was started by the safe insertion of the first resin plug defining the first dielectric boundary in the waveguide. Then the sand powder was carefully poured into the central section and evenly spread with the least amount of air gaps that could lower the accuracy of the measurement.

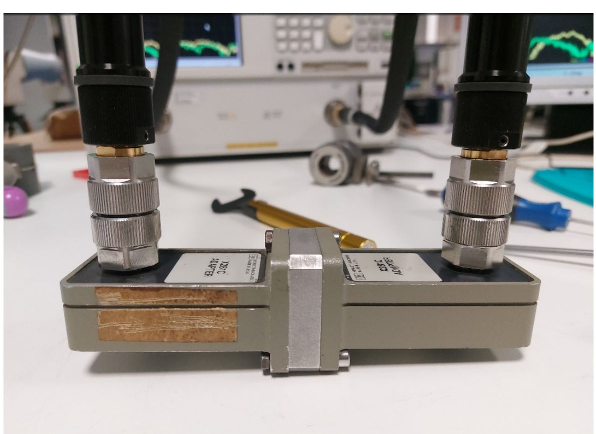

Figure 2. Measurement system

When the necessary layer thickness was achieved, the second resin plug was correctly placed in the specified position. This was carried out in order to keep the powder from being compacted to a thickness less than the nominal and to maintain uniformity of the sample.

The whole assembly procedure was designed to avoid leakage or external interference and to keep the sample stable, so that an accurate and repeatable dielectric characterization was possible. The complete measurement system is shown in Fig. 2.

Because of the symmetrical configuration of the measurement setup with the same resin plugs on both ends of the waveguide, the electromagnetic response at port 1 is identical to that at port 2. In this way, the reflection coefficient S_{11} is representative of both ports, and the calculation of S_{22} is ineffective in this context.

3.1 Direct Problem

3.1.1 Characterization of a Rectangular Waveguide with Resin Boundaries

A second configuration was studied in which the rectangular waveguide was closed at both ends with resin plugs to approximate the dielectric boundary conditions of the final test structure. The plugs were 1 mm thick and had a complex permittivity of $\varepsilon_r' = 3.1$ and $\varepsilon_r'' = 0.093$. The space between the plugs was still filled with air.

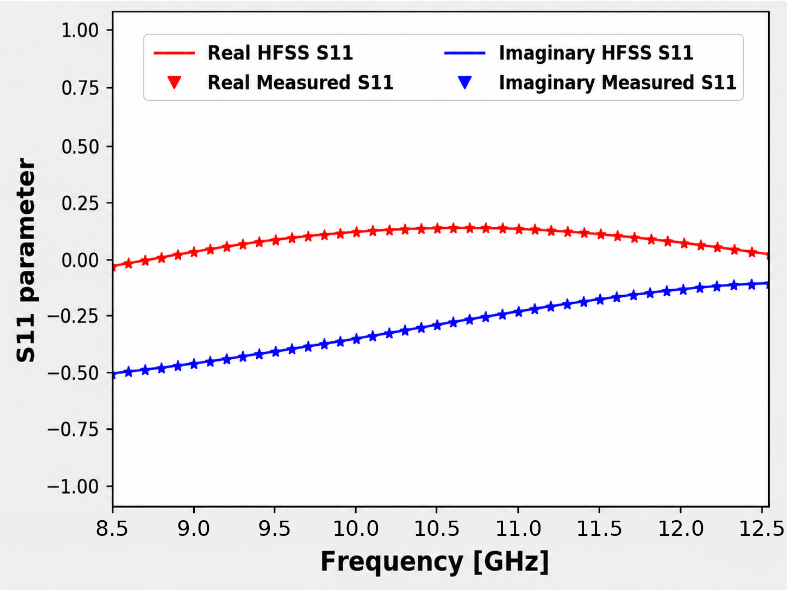

Figure 3. Reflection coefficient S_{11} for the waveguide with resin boundaries and an empty center

The calculated values of the reflection coefficient S_{11} are shown in Fig. 3, which are in very good agreement with the measured data, proving the reliability of the theoretical model. This confirms the correctness of the electromagnetic behavior introduced by the boundaries of the resin and the appropriateness of the configuration for the following analysis, where a dielectric material is inserted in the central section.

3.2 Inverse Problem

3.2.1 Estimation of Air complex permittivity in a Resin Bounded Rectangular Waveguide

Before filling the dielectric powder, a preliminary estimate of the complex permittivity of air was performed within a rectangular waveguide closed at both ends with resin plugs of known properties ($\varepsilon_r' = 3.1$, $\varepsilon_r'' = 0.093$). This step was done to verify the accuracy of the numerical model used in the following inversion steps.

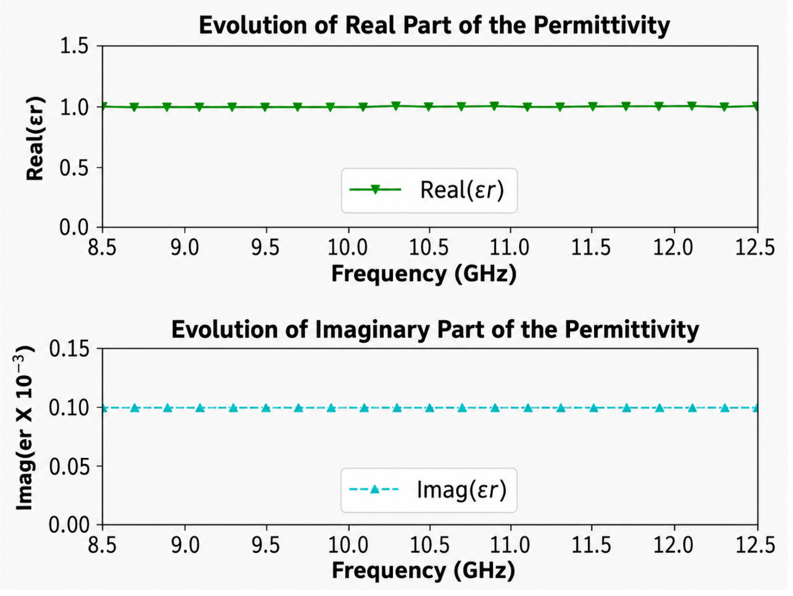

Figure 4. Estimated complex permittivity of air in a rectangular waveguide closed with resin plugs

The initial estimate of the complex permittivity of the air was taken as $\varepsilon_r' = 1.5$ and $\varepsilon_r'' = 0.005$, and iterative optimization was carried out to minimize the difference between the theoretical and measured $S11$ parameter. The model converged to values consistent with the expected low dielectric constant and negligible air loss. The results presented in Fig. 4 confirm the ability of the inversion procedure to reliably characterize low loss materials in the presence of dielectric boundaries.

3.2.2 Estimation of Powdered Sand complex permittivity

After validating the model with air, the sand was filled in the central region of the waveguide. An initial estimate of the complex permittivity of the sand has been introduced into the model, and an iterative algorithm has been used to refine the complex permittivity until the simulated S_{11} parameter has been matched with the measured data.

The results presented in Fig. 5 show the effect of the dielectric properties of the sand sample on the propagation of the wave and confirm the effectiveness of the inversion technique for powdered dielectric materials.

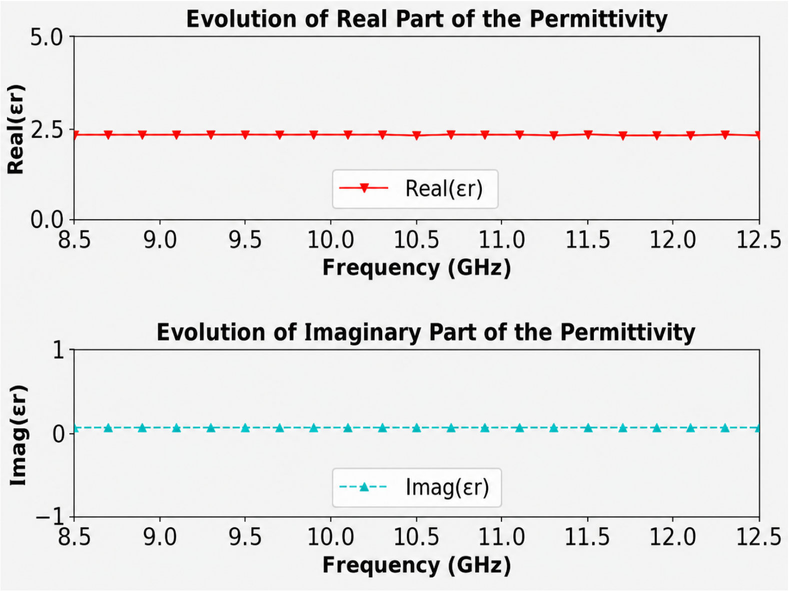

Figure 5. Estimated complex permittivity of sand in a rectangular waveguide closed with resin plugs

4 Conclusion

In the present work, a theoretical approach for the estimation of the complex permittivity of dielectric powdered materials embedded in a rectangular waveguide is presented. It was set up as a multilayer structure with two resin boundaries containing the sand sample with known layer thicknesses under controlled experimental conditions. The proposed method was able to characterize the dielectric properties of sand accurately and consistently by analytically formulating the direct electromagnetic problem and solving the inverse problem by numerical optimization. The measured reflection parameter (S_{11})was used to retrieve the real and imaginary parts of the complex permittivity in the X-band frequency range with high accuracy.

The results confirm the effectiveness and reliability of this fully theoretical technique and provide a robust and practical framework for the electromagnetic characterization of powdered materials in multilayer applications.

References

1. Hasar, U.C, Permittivity measurement of thin dielectric materials from reflection-only measurements using one-port vector network analyzers. *Prog. Electromagn. Res.* **95**, 365-380 (2009). https://doi.org/10.2528/PIER09062501
2. Talmoudi, O., Benali, L.A., Terhzaz, J., Tribak, A., Fernández-Ibáñez, T, A novel hybrid 2D-FDTD-PML and Nelder-Mead methods for estimating liquid complex permittivity using a rectangular waveguide. *J. Appl. Phys.* **137**(14) (2025). https://doi.org/10.1063/5.0264173
3. Sharma, A., Afsar, M.N, Microwave complex permeability and permittivity of nanoferrites. *J. Appl. Phys.* **109**, 07A503 (2011). https://doi.org/10.1063/1.3536659

4. Qin, J., Liu, Z., Ma, M., Li, Y, Machine learning approaches for permittivity prediction and rational design of microwave dielectric ceramics. *J. Materiomics* **7**(6), 1284-1293 (2021). https://doi.org/10.1016/j.jmat.2021.02.012
5. Xu, J.D., Fang, H.R, Permittivity extraction using waveguide transmission method in x-band for powder materials. *IEEE Access* **8**, 105421-105428 (2020)
6. Soliman, A.H.S., Abd El-Rahman, M.H, Accurate technique for complex permittivity measurement using rectangular waveguide in x-band. *IEEE Trans. Instrum. Meas.* **70**, 1-8 (2021)
7. Nelder, J.A., Mead, R, A simplex method for function minimization. *Comput. J.* **7**(4), 308-313 (1965). https://doi.org/10.1093/comjnl/7.4.308
8. Hasar, U.C., Cansiz, A, Simultaneous complex permittivity and thickness evaluation of liquid materials from scattering parameter measurements. *Microw. Opt. Technol. Lett.* **52**(1), 75-78 (2010). https://doi.org/10.1002/mop.24837
9. Ebara, H., Inoue, T., Hashimoto, O, Measurement method of complex permittivity and permeability for a powdered material using a waveguide in microwave band. *Sci. Technol. Adv. Mater.* **7**(1), 77-83 (2006). https://doi.org/10.1016/j.stam.2005.11.019
10. Hotta, M., Hayashi, M., Lanagan, M.T., Agrawal, D.K., Nagata, K, Complex permittivity of graphite, carbon black and coal powders in the ranges of x-band frequencies (8.2 to 12.4 GHz) and between 1 and 10 GHz. *ISIJ Int.* **51**(11), 1766-1772 (2011). https://doi.org/10.2355/isijinternational.51.1766
11. Virtanen, P., Gommers, R., Oliphant, T.E., Haberland, M., Reddy, T., Cournapeau, D., et al. SciPy 1.0: fundamental algorithms for scientific computing in Python. *Nat. Methods* **17**, 261-272 (2020). https://doi.org/10.1038/s41592-019-0686-2
12. Talmoudi, O., Benali, L.A., Terhzaz, J., Tribak, A., Fernández-Ibáñez, T, Determination of distilled water dielectric constant by 2D-FDTD method at x-band frequencies. In: *IRASET*, IEEE, June 2024. https://doi.org/10.1109/IRASET60544.2024.10549156